

UDK: 53.086; 669.018; 669.14

## The Investigation of the Effect of Cu Addition on the Nb-V Microalloyed Steel Produced by Powder Metallurgy

Mehmet Akif Erden<sup>1\*)</sup>, Ahmet Mustafa Erer<sup>2</sup>, Çağrı Odabaşı<sup>3</sup>, Süleyman Gündüz<sup>2</sup>

<sup>1</sup>Karabük University, Engineering Faculty, Biomedical Engineering Department, Karabük

<sup>2</sup>Karabük University, Science Faculty, Physics Department, Karabük

<sup>3</sup>Karabük University, Graduate School of Natural and Applied Sciences, Manufacturing Engineering Department, Karabük.

<sup>4</sup>Karabük University, Technology Faculty, Manufacturing Engineering Department, Karabük.

---

### Abstract:

*In this work, the effect of Cu content on the microstructures, mechanical properties and electrical conductivity of Nb-V added microalloyed powder metallurgy (PM) steels were investigated. Microalloyed steel samples were pressed at 750 MPa and sintered at 1400°C in argon atmosphere for 1 h. The grain size and phase distribution of the microalloy steels were determined by optical microscope. The precipitates and fracture surface of samples were analyzed with the help of SEM and EDS analyses. Tensile test, hardness test and electrical conductivity measurement were carried out for the Nb-V added microalloyed steel with different Cu content. Results indicated that 10 wt.% Cu added PM microalloyed steel showed the highest values in yield strength (YS) and ultimate tensile strength (UTS). However, when the amount of Cu content increased from 10 to 15 wt.%, YS and UTS decreased. Elongation also tends to decrease with increasing Cu content. Although the electrical conductivity in general increased with the addition of Cu, a decrease in some conductivity was observed in the addition of 15 wt.% Cu.*

**Keywords:** Powder metallurgy; Nb-V microalloyed steels; Microstructure; Mechanical properties; Electrical conductivity..

---

## 1. Introduction

Microalloyed steels contains precipitation forming elements such as Ti, V, Nb and Al which are added less than 0.2 wt.% for increasing the mechanical properties of steel. The main roles of microalloying elements are to refine the grain size, prevent recrystallization and facilitate precipitate hardening occurred through carbide and nitride precipitates. Due to the small amount of alloy, they are lighter in weight and cheaper in terms of cost. Production opportunities are also faster, so the losses in terms of time and energy are less. Microalloyed steels have been used in many places such as pressure vessels and storage tanks [1-3].

Vanadium forms as VC, VN or V<sub>2</sub>C (N) precipitates that have lower solubility compared to the Fe<sub>3</sub>C and thus, the undissolved precipitates prevent grain growth and

---

\*) Corresponding author: makiferden@karabuk.edu.tr

recrystallisation resulted of good mechanical properties of microalloyed steels. These steels are resistant to annealing up to about 600°C. The drastic reduction of hardness is caused by the decomposition of Fe<sub>3</sub>C during annealing, and even very small amounts of V reduce the susceptibility of the steel to overheating as it produces hardly soluble carbides. Nb is very effective in preventing recrystallisation of the austenite and producing fine ferrite grains compared to V. Nb is widely used in this way for the production of fine grained structural steel. This depends on the amount and size of the deposited NbC and the addition of 0.01 % Nb increase the strength of 35-40 MPa. The Nb, Ti and V are now widely used to increase the toughness and strength of structural steel [4]. Cu powder is added to the Fe powder in order to increase the strength of the sintered metal. During the sintering of Cu-Fe metal, dimensional changes occur due to the percentage of Cu and pure Fe parts usually shrink during sintering. By adding increasing amounts of Cu powder and sintering above the melting temperature of the Cu (1083°C), this shrinkage is reversed and consequently converted to expansion. The expansion increases in parallel to the amount of Cu increasing up to 8 -10 wt.% Cu, which is dependent on the solubility limit in Fe and decreases after this value. A small amount of Cu (2 wt.%) can be used to compensate for the shrinkage of pure Fe samples during sintering [5]. By adding both Cu and C together to the Fe powders, the higher strength and hardness values are obtained compared to the addition of these alone. The addition of graphite to the Fe-Cu mixtures reduces the expansion of Cu during sintering. The addition of Cu to the Fe-C mixtures also tends to reduce the dependence on the atmosphere quality. In other words, the addition of Cu helps to prevent decarburization in decarburizing atmospheres [6-7].

Although PM is not a new known process, it has been used as an industrial process in the early 20th century and is widely used in the developed countries of the world and its products find wide application areas in the industry. All known metal mixtures can be prepared by the PM method to produce the desired composition, such as non-machining parts, hard metals, tool steels, self-lubricating bushings, friction elements, electrical contact materials, graphite brushes and magnets. The parts produced by this method have a less rough surface than the parts produced by other methods and often do not require secondary processing. Homogeneous distribution of the quality, completely controllable ingredient and content, and low unit cost make powder metallurgy as a unique production method in the production industry [8-13]. Thus, it was found that approximately 97 % of the material was used in mass production with PM. In this direction, the piece is cheaper and easily produced in the desired composition [13].

Microalloyed steels today are nowadays produced in the form of pipe and sheet by conventional steel production method. Also, microalloyed steel is being produced by PM method although the production is not enough. In the literature, there are some studies about the relationship between microstructure and mechanical properties of microalloyed steel produced by PM method. For instance, in their study, Erden et al. [1] produced a Ti microalloyed steel via PM method. It is observed that increasing Ti content (by weight 0-0.1-0.15 % and % 0.2) increased YS and UTS which is attributed to the formation of TiC(N) precipitates during cooling period after sintering. They showed that, precipitates like TiC, TiN and TiCN prevents grain coarsening and leads to formation of little austenite grains which, in order, improve the strength of material. Turkmen et al. investigated the effects of heat treatment on the microstructures and mechanical properties of powder metallurgy (PM) Nb-V microalloyed steels (Fe + 0.25%C + 0.075%Nb + 0.075%V). Experimental results showed that microalloyed steels can be produced by PM technology and the heat treatment affects the microstructure and mechanical properties of microalloyed PM steel [14]. Özdemirler et al. [15] also investigated the effect of sintering temperature on microstructure and mechanical properties of NbC added PM steels. They found that the precipitation of NbC limits grain growth that results in significant improvement in strength.

In this study, the effect of Cu addition in the range of 0.5-15 wt.% on microstructures, mechanical properties and electrical conductivity of Nb-V added microalloyed PM steel was

examined. For this purpose, the mixed powders were pressed in a mould under 750 MPa pressure as tensile test samples which were then sintered at 1400°C in an atmosphere-controlled furnace.

## 2. Materials and Experimental Procedures

In this study, graphite, Nb, V and Cu powders supplied Aldrich and Höganas were used to fabricate steel specimen. The size of graphite, Fe, Nb, V and Cu powders are <20, ≤180, <45, <44 and <75µm respectively. The purities of graphite, Fe, Nb, V and Cu are 96.5 %, 99.9 %, 99.8 %, 99.5 % and 99 %, respectively. Fig. 1 shows SEM micrographs of the powders subjected to hydrogenation and milling. When the SEM image of the iron powder is examined in Fig. 1, it is seen that clumping, saturation and carbon dusts are hazy. Nb, V and Cu powders have been angularly shaped as a result of hydrogenation and milling under vacuum.

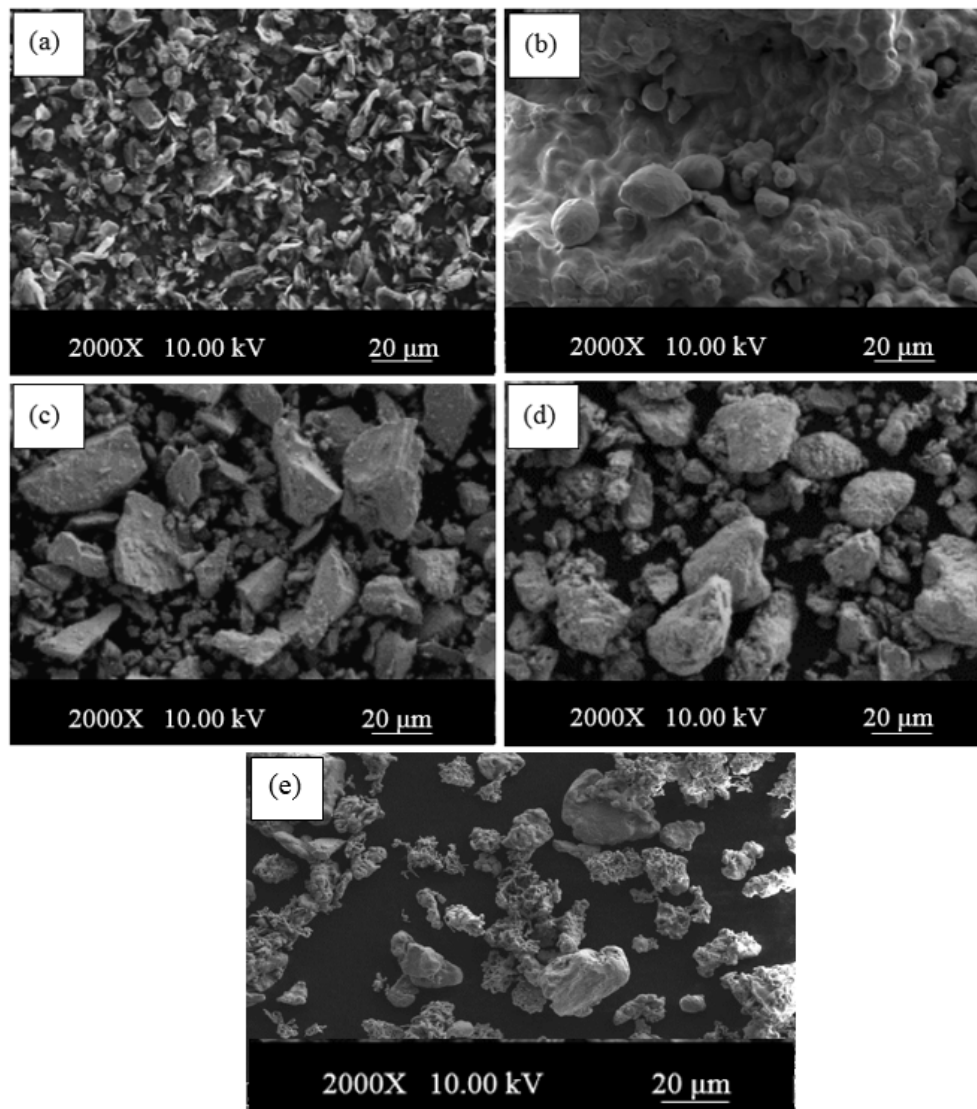


**Fig. 1.** SEM images of powders; (a) graphite (2000X), (b) Fe (2000X), (c) Nb (2000X), V (2000X) and Cu (2000X).

For producing the alloyed steel specimens with the combinations given in Table I, the powders were accurately weighed and mixed in a TURBULA T2F device for 1 h. without ball. The mixed powders were unidirectional pressed to tensile test specimen according to ASTM E8/E8M [16] under 750 MPa pressure by using hydraulic press. Tensile test specimens were produced by powder metallurgy route with the compositions given in Table I (Alloy 1-5).

**Tab. I** Chemical compounds of powder metal steels.

Compositions	Graphite (%wt.)	Nb (%wt.)	V (%wt.)	Cu (%wt.)	Fe (%wt.)
Alloy 1	0,25	-	-	-	Rest
Alloy 2	0,25	0,075	0,075	-	Rest
Alloy 3	0,25	0,075	0,075	0,5	Rest
Alloy 4	0,25	0,075	0,075	5	Rest
Alloy 5	0,25	0,075	0,075	10	Rest
Alloy 6	0,25	0,075	0,075	15	Rest

The pressed tensile test specimens were sintered at 1400°C in a tube furnace with an argon atmosphere. Sintering process was started by heating up the specimens to the sintering temperatures at a rate of 5 °C/min and kept at this temperature for an hour before cooling down to environmental temperature by a cooling rate of 5 °C/min. Fig. 2 shows tensile test specimens which were subjected to electrical conductivity, tensile and hardness tests. Densities, volume fraction of ferrite and pearlite and grain sizes of the specimens were also determined.



**Fig. 2.** General view before and after tensile tests specimen obtained from Alloy 2 sintered at 1400°C.

A SHIMADZU hardness measuring device was used to measure the microhardness of all the non-alloyed and microalloyed specimens under HV0.5 (500g) load. Hardness value of the specimens was determined by the average value of 10 measurements taken for each specimen. Tensile test was carried out at 1 mm/min crosshead speed by using a SHIMADZU (with 50 kN capacity) tensile testing machine. Stress-strain diagrams were obtained, from which YS (0.2 %), UTS and percent elongation values were calculated.

Densities of the specimens were determined by Archimedes principle using pure water according to ASTM B 328-96 [17]. Microstructural studies were carried out using optical and scanning electron microscopes (SEM). The microstructures were examined in a Nikon L150 model microscope with magnification of max. 1000 X. Grain sizes of non-alloyed and alloyed PM steels were calculated by using mean linear intercept technique on the optical micrographs [18]. Volume fractions of phases of the specimens are calculated by metallographic point counting method explained by Gladman and Woodhead [19].

Electrical conductivity measurement test was also carried out to examine the mechanisms responsible for precipitation. When current (I) is applied to a conductive

material, the potential difference ( $V$ ) between the ends of the conductor is measured. The resistance of the material is equal to ( $R$ ) ( $V/I$ ) in which  $R$  is directly proportional to the length ( $L$ ) of a conductor and inversely proportional to the cross-sectional area ( $A$ ) as given in equation 1:

$$R = \rho L/A \quad (1)$$

where ( $\rho$ ) is the resistivity in ohm which affect the material resistance. In the resistivity measurement method, it is possible to measure the potential difference in the material surface associated with a known current flow and thus to calculate the resistivity value [20].

### 3. Results and Discussion

SEM microstructure of the samples given in Fig. 3 showed that the structures of Alloys 1, 2 and 5 consist of ferrite and pearlite phases in different volume fractions with NbC and VC precipitate particles which prevented grain growth.

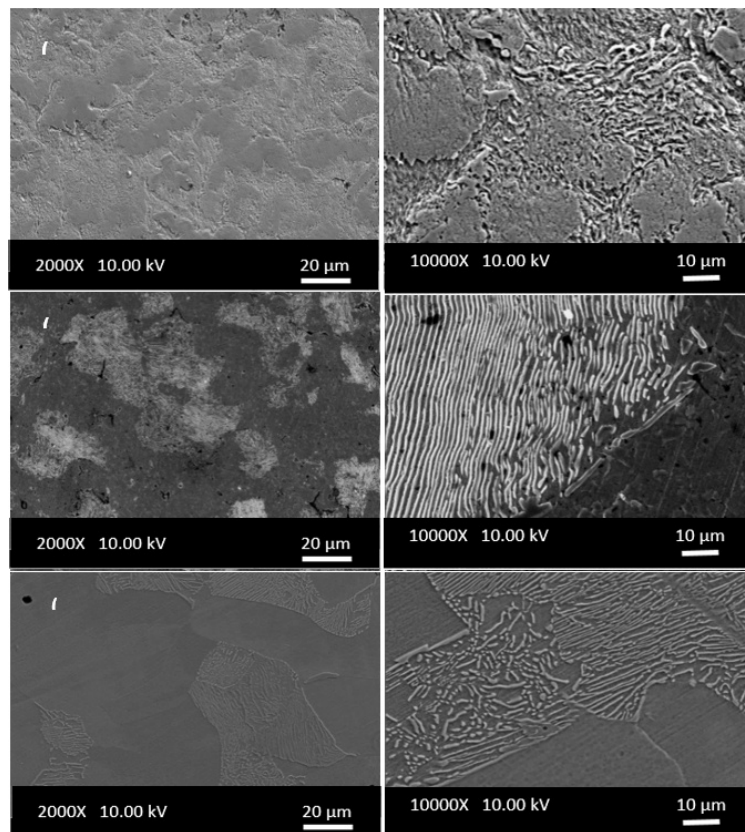


**Fig. 3.** SEM microstructure images of steel samples produced by the PM method X2000-X10000; (a) Alloy 1, (b) Alloy 2 and (c) Alloy 5.

Table II also shows relative density, porosity (%), pearlite (%) and grain sizes of Alloys 1-6. As can be seen that the addition of Cu up to 10 wt.% reduces the grain size and increases the amount of pearlite. However, further increase in Cu content to 15 wt.% caused a decrease in pearlite amount and grain refinement because of the excessive accumulation of Cu in the grain boundaries. Özgün [21] observed an increase in the pearlite amount but a decrease in

grain sizes with the addition of Cu into the material. The presence of Nb and V microalloying elements in Alloys 1-6 provides the formation of carbide and nitrides which prevent grain growth during sintering or cooling after sintering. The formation of small precipitates during austenitization prevents the growth of austenite grains and provide the formation of small ferrite grains during cooling [18]. Cu can cause precipitate strengthening without C and N. Mean while its precipitated phase is in nanometer size, Cu may be precipitated more thinly than carbides or nitrides such as Nb (C, N) and may produce finer grain sizes [22-25]. At the same time, Cu clusters and precipitates can also be used. Sintering density of Alloys 1-6 is seen in Table II. Density, being an important parameter in powder metallurgy, effects mechanical properties in a smuch as the residual voids created after sintering fall down the strength, cooling rate of the material. These voids are critical for the initiation and distribution of cracks [26-27]. Formability and toughness are much more dependent on density. When the density is high, formability and toughness increase [27]. However, density values all of them are similar in general (92 %) after sintering. In addition, when the density values were compared, it was close to each other in all alloys, but also the composition containing 10 % Cu (Alloy 5) of the densest compound. As it is known, the increase in density contributes to the strength. It is observed that the addition of up to 10 % by weight of copper in the amount of particle reduces the grain size and causes the increase in perlite amount. Many studies on grain-refinement and ingreasing hard phaseof Cu additon in steels have been carried out [28-32]. For examples Takaki at al. [28], have studied the effect copper on grain-refinement of steel. They have claimed that along with a change in the microstructure ferrite pearlite for Cu free steel to ferrite-marten site for high Cu added steel. Evans and Coworkers [33] has studied the effect of copper in C-Mn steel weld metal deposits. They have found that increasing copper content, a general decrease in acicular ferrite (AF) content, increase in ferrite with second aligned phase and promotion of hard phases and refinement of microstructure. Yi et al. [32] have indicated that as increasing of copper concentration, the morphologies of matrix have changed from pearlite and a little ferrite have appeared and the ferrite tends to disappear later Surprisingly, a few large clusters of pearlite colonies are observed besides the individual pearlite colonies.

**Tab. II** Relative density (%), porosity (%), pearlite (%) and grain sizes of Alloys 1-6.

Compositions	Relative Density(%)	Porosity (%)	Pearlite (%)	Grain Size ( $\mu\text{m}$ )
Alloy 1	93.30	6.70	22.9	34.5
Alloy2	93.40	6.60	24.7	30.2
Alloy3	93.25	6.65	26.7	24.1
Alloy4	92.70	8.10	38.8	22.5
Alloy5	93.90	5.90	42.2	21.1
Alloy6	91.10	9.90	28.3	26.9

SEM and EDS analysis results of 1400°C sintered Alloy 1 produced by PM method can be seen in Fig. 4. It is seen from Fig. 4 that nonalloyed Alloy 1 showed  $\text{Fe}_3\text{C}$  with different dimensions according to SEM and EDS analyses results. When Nb-V added microalloyed steels containing Cu in different percentages were examined, it was observed that NbC (N) and VC (N) precipitates were formed in steel. It indicated that these precipitates prevent the austenite grain growth and also increase the strength of the material by precipitation hardening [34].

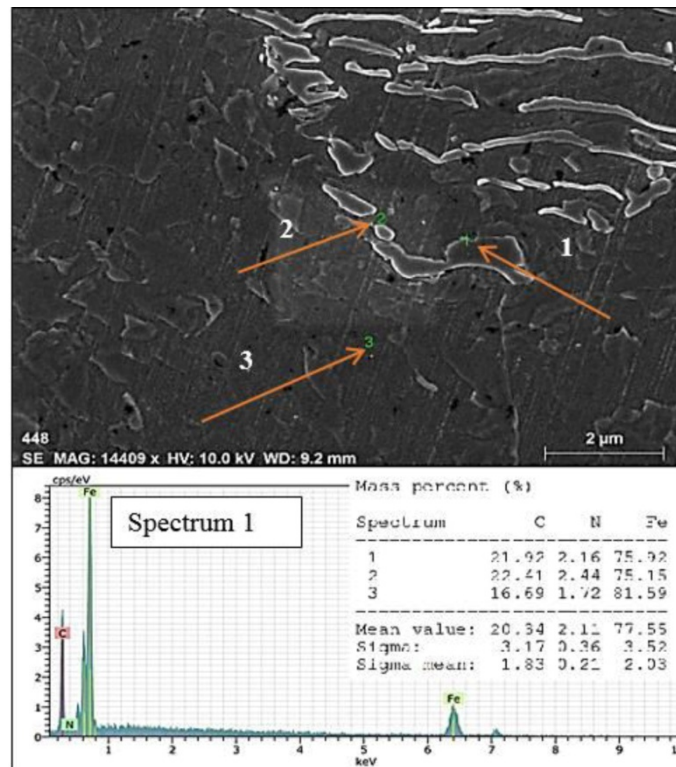


Fig. 4. SEM micrograph for Alloy 1 and corresponding EDS of the indicated points.

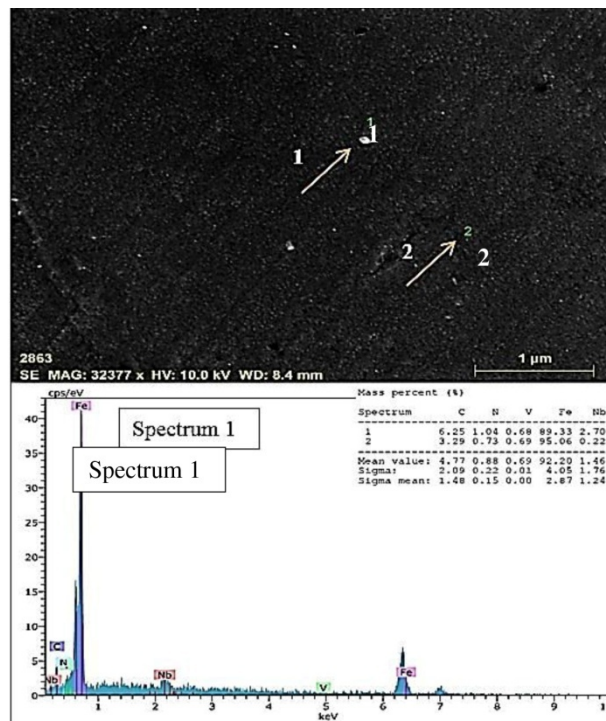
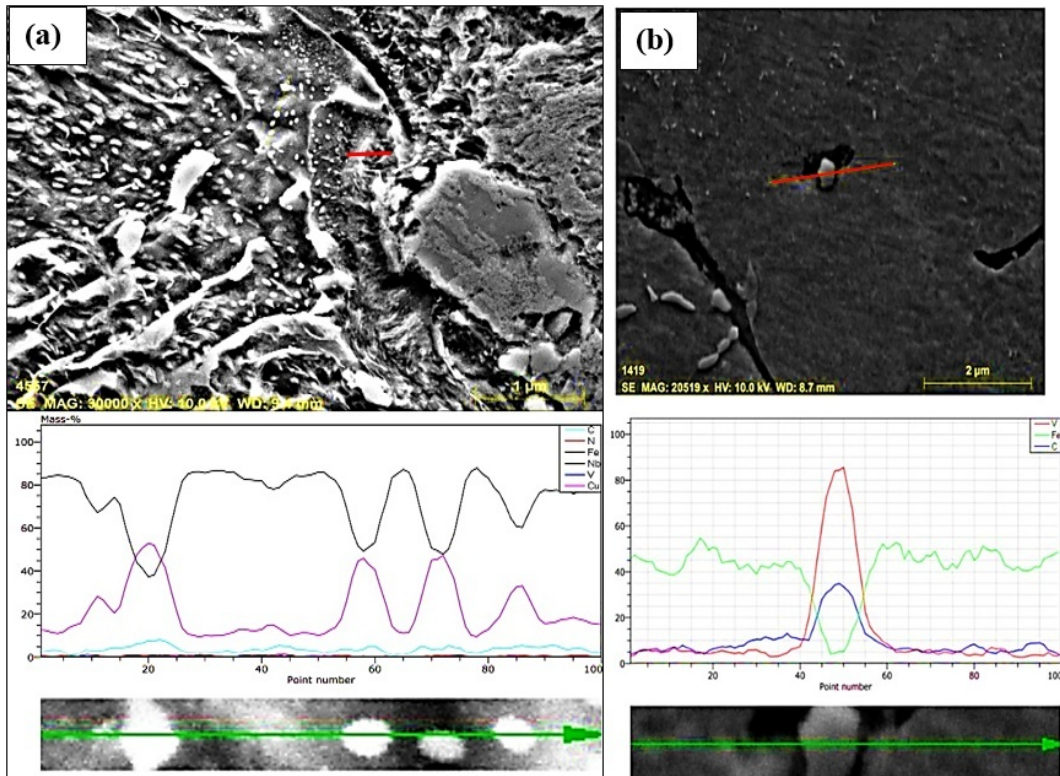


Fig. 5. SEM micrograph for Alloy 2 and corresponding EDS of the indicated points.

Fig. 5 shows SEM and EDS analysis results of Alloy 2 containing microalloying elements of Nb and V. SEM and EDS analyses indicated that NbC(N) and VC(N) with different sizes

occurred in Alloy 2 during sintering or cooling after sintering. Siwecki et al. [35] investigated the precipitation behavior of low carbon microalloyed steel containing Ti and V. They indicated that both TiN, VN or Ti,V(N) precipitates formed in austenite phase and inner part of precipitate is rich in Ti and the outer part is rich in V which means that V precipitates onto TiN to form Ti,V(N). Fig. 5 exhibited that EDS point analysis taken from the precipitate contained both V and Nb, and the amount of carbon is clearly higher when compared to EDS point analysis taken from the matrix. It is thought that this precipitate could be Nb,V(C). When EDS analyses results obtained from this study were compared with literature, it indicated that precipitates like VC(N) and NbC(N) occurred in microalloyed PM steels.

Fig. 6a and 6b also shows EDS line analyses of the cross section of the matrix and precipitate particles in Alloy 5 containing V, Nb and Cu elements. Concentration distribution of V, Nb and Cu elements along the line can be seen in Fig. 6. As can be seen, type and the amount of element in Alloy 5 sintered at 1400°C vary along the line intersecting the matrix and precipitates. It is determined that matrix phase is rich in iron however; spherical precipitate is rich in niobium. Besides, there is a sharp increase in amount of copper (Figure 6a) and vanadium (Fig. 6b) from Fe rich matrix to round shape particle, while Fe showed inverse behavior. The presence of this phase showed that VC (Fig. 6a) and Cu (Fig. 6b) particles occurred during sintering or cooling after sintering. Moreover, when the copper addition exceeds 2 wt% in alloys, the solubility of copper in alloy 3 will exceed the critical solubility of copper in alloys [30]. Thus, the particles in alloy 4-5-6 should be the Cu nano precipitations. In order to further recognize the Cu-rich precipitation in  $\alpha$ -Fe, the morphology of nano Cu-rich precipitation are detected using SEM in Fig. 6a.



**Fig. 6.** SEM micrograph for Alloy 5 sintered at 1400°C and EDS lines scan of the indicated particle.

Fig. 7 and Table III show mechanical test results of Alloys 1-6 by giving YS, UTS, percentage elongation and hardness values. As is seen, Alloy 1 which does not contain any

alloying elements exhibited the lowest mechanical properties compared to the Alloys 2-6. However the effect of the alloying elements in Alloy 2-6 is clearly seen with the increase of YS and UTS. This is due to the precipitation of microalloying elements and finer grain size which provide an increase in mechanical properties. This is consistent with the results obtained by Erden et al. [1] and Erden, [4,26] who produced PM steel by adding microalloying elements such as Nb, V and Ti in their studies. They observed that the YS, UTS and hardness of the steel increased and the grain size decreased by the addition of microalloying elements. This is due to the precipitation of carbonitrides such as NbC(N), VC(N) and TiC(N) during sintering or cooling after sintering. These precipitate particles prevented grain growth of austenite grains and increased the strength by precipitation hardening, dispersion hardening or grain refinement mechanisms.

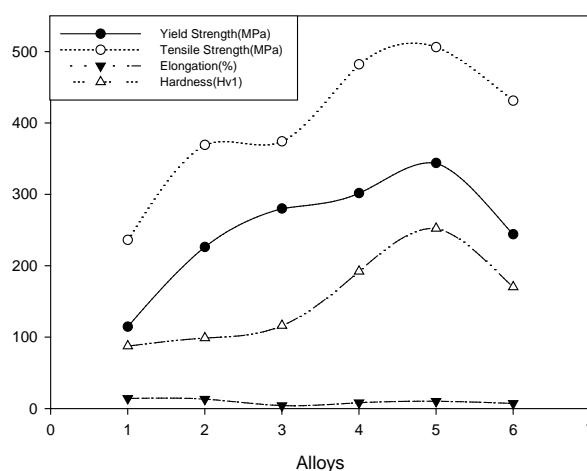


**Fig. 7.** Mechanical properties of Alloys 1-6.

In the present experimental work, Alloys 2-6 were produced for the same weight percentage of microalloying elements of Nb and V, but different weight percentage of Cu in order to compare the effect of the Cu addition on the mechanical properties of Alloys. The addition of Cu continuously increased strength but decreased the percentage elongation of Alloys up to 10 wt.% Cu addition. The highest yield strength, tensile strength and hardness but the lowest percentage elongations were obtained in Alloy 5 with 10 wt.% Cu addition. This is consistent with the study of Uygur [30] who observed an increase in the YS and UTS of samples when the amount of Cu was increased from 1 wt.% to 2 wt.%. It is thought that this increase in strength is due to the fact that Cu is deposited in the grain and grain boundaries which decreased the grain size and increased the amount of pearlite. Among different precipitation-strengthened ferrite alloys, the Fe–Cu system is probably the most studied one. The hardening effect arising from Cu-rich precipitates has been known for a long time. Similar results were obtained in other study carried out by Özgün [21]. He showed an increase in the amount of pearlite by the addition of Cu in the material. Takaki et al. [28], Zhou et al. [36], Wen et al. [37] and Uygur [30] have reported that Cu in steels can be contributed to strengthening in steels. Owing to Cu precipitated as fine dispersed Cu-rich phase particles, which has excellent dispersion strengthening effect. Takaki et al. [28] have claimed that Cu clusters might contribute to strengthening without deteriorating ductility because Cu clusters are softer than carbides. In this study, it is clear that while 0.2 mass% Cu steel showed low and almost constant hardness, 1.0 mass% Cu steel exhibited higher hardness and even showed peak aging phenomenon. It was also found that hardness increased with increasing Cu content. However, a decrease in strength was observed when the Cu addition was increased to 15 wt.%. The reason for this is the excessive accumulation of Cu at the grain boundaries

which caused the loss of grain refinement and a decrement in pearlite amount. Indeed, Özdemirler et al. In the study, he produced micro alloy steel and observed that the addition of Nb after certain ratio decreased the strength. The reason for the decrease in strength was attributed to the excessive accumulation of the Nb element at the grain boundaries [15].

**Tab. III** Yield strength, tensile strength, hardness and percentage elongation values of Alloys 1-6.

Alloy	Yield Strength (MPa)	Tensile Strength (MPa)	Elongation (%)	Hardness (Hv <sub>1</sub> )
1	114,5	236	14	87,3
2	226,1	369	13	98,6
3	280	374	14	116
4	301,5	482	8	192
5	343,7	506	10	252
6	244	431	7	170

Fig. 8 shows electrical conductivity change for Alloys 1-6. The electrical conductivity of the Alloys 1-6 were measured by using starting and ending voltage values of 0.001-0.01V for 0.1 delay time in the KEITHLY 6482 DUAL-CHANNEL brand machine. Electrical conductivity measurements provide a significant indication for the precipitation of carbonitrides in Alloys 1-6 obtained by the addition of Nb, V and Cu. It is seen from Fig. 8 that Cu addition increases the electrical conductivity which showed that large amount of Nb, V or Cu atoms were precipitated out of solution. Gündüz and Kaçar [38] measured microhardness and electrical conductivity of 6063 Al alloy to investigate the mechanisms responsible for artificial ageing. They observed an increase in electrical conductivity due to precipitation of larger size particles. However, when the Cu content was increased to 15 wt.% (Alloy 6), a decrease in conductivity was observed. The reason for this is the increase in CuO and volume fraction of porosity [39].

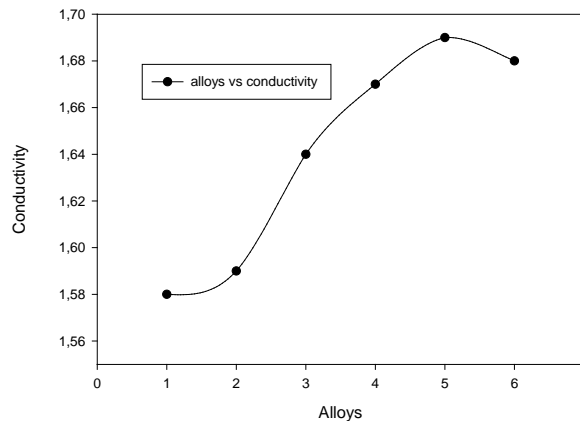


**Fig. 8.** Electrical conductivity values of Alloys 1-6.

Fig. 9 shows the fracture surfaces of the Alloys 1, 2 and 5 after tensile testing. Changes were observed on the fracture surfaces of the alloys with respect to the shape, size and depth of the microvoids. As is seen from Fig. 9 that fracture surfaces are partially ductile (honeycomb structure) and partially brittle (cleavage plane). Voids are evident throughout the whole fractured surface. This indicates that fracture propagate by the formation of voids and

coalescence in the necks between adjoining fracturing microvolumes. However, cleavage planes, which is an indication of brittle fracture, are the most prominent in the Alloy 6 containing 15 wt.% Cu, quite prominent in Alloys 3-5 containing 0.5-10 wt.% Cu, and the least prominent in the Alloys 1 and 2 which does not contain Cu element. Alloy 5 also showed large voids which are an indication of the removal of NbC or VC precipitates from the fracture surface. This indicates crack tip bridging mechanisms in Alloy 5. M. Hajisafari et al. [40] indicated that nucleation and growth of voids in microalloyed steel depend on the mismatch between the second-phase particle and the metal matrix. Voids firstly nucleate around second phase particles and consequently grow.

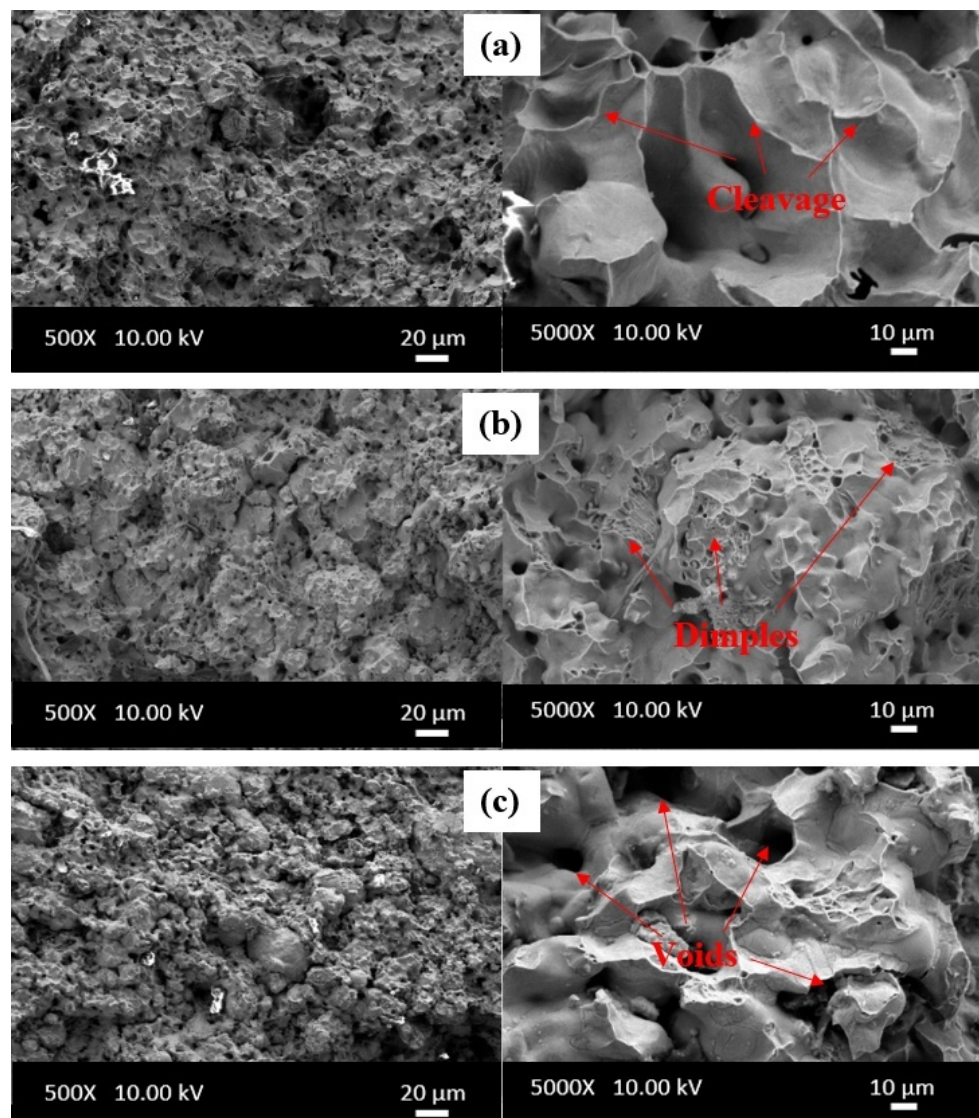


**Fig. 9.** Fracture surfaces of alloys sintered at 1400°C: (a) Alloy 1, (b) Alloy 2 and (c) Alloy 5.

The Cu-O based particle in fracture surface of Alloy 6 which shows a decrement in electrical conductivity was also observed in the SEM fractograph and the corresponding EDS results in Fig. 10. This explains the decrement in electrical conductivity of Alloy 6 with the addition of Cu in the weight percentage of 15 %.

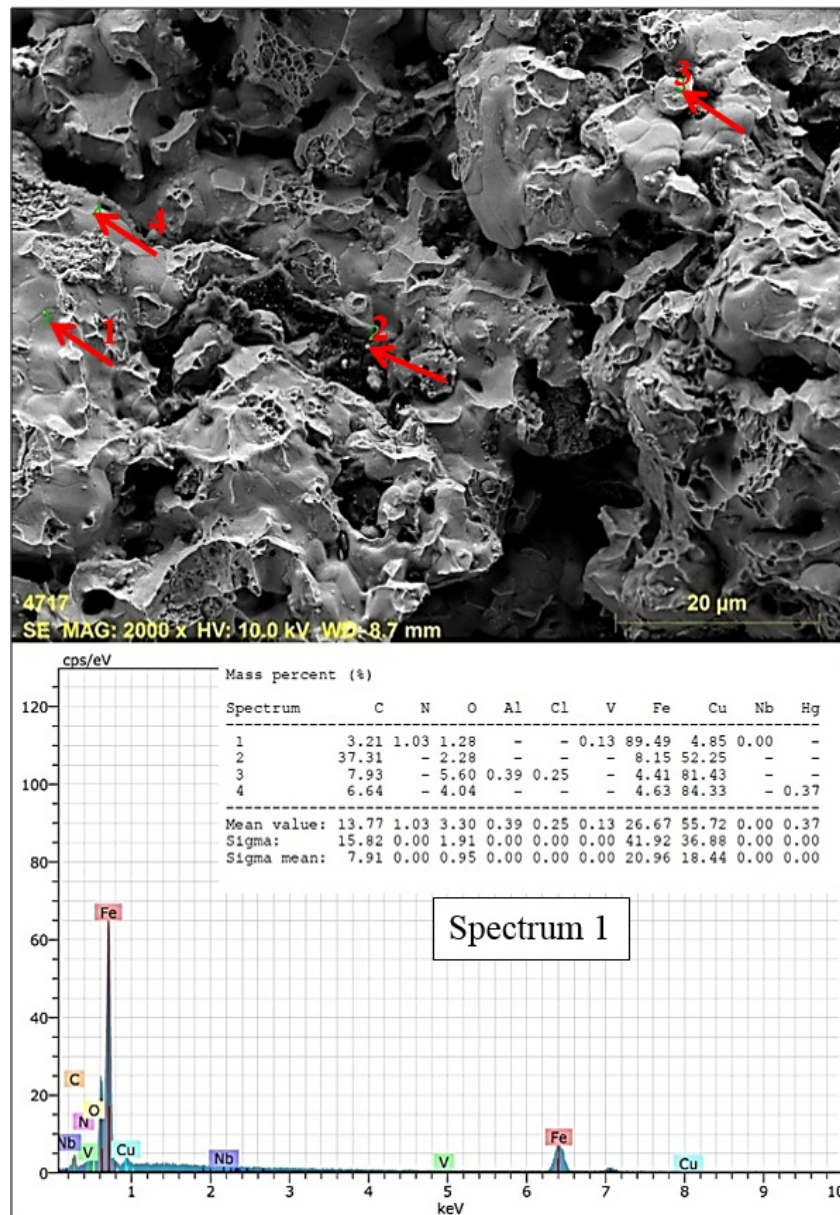


Fig. 10. EDS results from the indicated particle of Alloy 6.

#### 4. Conclusion

In this study, the influence of Nb, V and Cu addition on mechanical properties and electrical conductivity of PM steel sintered at 1400°C in argon atmosphere were studied. The results listed below were obtained from this study.

- 1- Nb, V and Cu added alloys (Alloys 2-6) exhibited smaller grain sizes than unalloyed steel (Alloy 1). This is due to the fact that carbides and nitrides formed by alloying elements prevent grain growth.
- 2- The addition of Cu continuously increased strength but decreased the percentage elongation of Alloys up to 10 wt.% Cu addition. The highest YS, UTS and hardness but the lowest percentage elongation were obtained in Alloy 5 with 10 wt% Cu

addition. However, a decrease in strength was observed when the Cu addition was increased to 15 wt.%. The reason for this is the excessive accumulation of Cu at the grain boundaries which caused the loss of grain refinement and a decrement in pearlite amount.

- 3- 3-Cu addition up to 10 wt.% increases the electrical conductivity which showed that large amount of Nb, V or Cu atoms were precipitated out of solution. However, when the Cu content was increased to 15 wt.%, a decrease in conductivity was observed. The reason for this is the increase in CuO and volume fraction of porosity.
- 4- Changes were observed on the fracture surfaces of the alloys with respect to the size, shape and depth of the microvoids. Fracture surfaces of alloys are partially ductile (honeycomb structure) and partially brittle (cleavage plane). However, cleavage planes, which is an indication of brittle fracture, are the most prominent in the Alloy 6 containing 15 wt.% Cu, quite prominent in Alloys 3-5 containing 0.5-10 wt.% Cu, and the least prominent in the Alloys 1 and 2 which does not contain Cu element.

## Acknowledgments

This work was supported by Scientific Research Projects Coordination Unit of Karabük University (Karabük, Turkey). Project Number: KBÜBAP-18-YL-017, KBÜBAP-18-DS-180 and KBÜBAP-17-YL-178.

## 5. References

1. M. A. Erden, S. Gündüz, M. Türkmen, H. Karabulut, *Materials Science and Engineering A*, 616 (2014) 201-206.
2. Gündüz, S., Erden, M. A., Karabulut, H., Turkmen, M., *Powder Metallurgy and Metal Ceramics*, 55(5-6) (2016) 277-287.
3. M.A.M. Ahssi, M. A. Erden, M. Acarer, H. Çuğ, *Materials*, 13 (2020) 4021.
4. M. A. Erden, *Metals*, 7 (2017) 329.
5. Höganäs, A. B., "Production of iron and steel powders", chapter 2, 3-21s, Höganäs PM School, (1996).
6. M. Spasojević, S. Randić, A. Maričić, T. Trišović, M. Spasojević, *Science of Sintering*, 52 (2020) 109-121.
7. A. Ataş, Investigating the mechanical properties of alloyed iron powder compacts after sintering", Master Thesis İstanbul University Natural and Applied Science Department of Metallurgy and Materials Engineering, İstanbul, Turkey (2003).
8. A.Güral, O.Altuntaş, *Materials Chemistry and Physics*, 259,(2021), 124203.
9. M. Akkaş, S. Islak, *Science of Sintering*, 51 (3) (2019) 327-338.
10. M. Akkaş, F. R. Abbood Al Sudani, *Science of Sintering*, 53(2021)19-35.
11. Y. Kaplan, S. Aksöz, H. Ada, E. İnce, S. Özsoy, *Science of Sintering*, 52(2020) 445-456.
12. M. Taştan, H. Gökozan, P. S. Çavdar, G. Soy, U. Çavdar, *Science of Sintering*, 52(2020) 77-85.
13. M. A. Erden, F. Aydın, *Int. J. Miner. Metall. Mater.*, 28(3) (2021), 430-439.
14. M. Türkmen, M. A. Erden, H. Karabulut, S. Gündüz, *Acta Polonica A*, 135(4) (2019) 834-836.
15. D. Özdemirler, S. Gündüz, M. A. Erden, *Metals*, 7 (2017) 121.
16. ASTM E8/E8M. Standard Test Methods for Tension Testing of Metallic Materials; ASTM International: West Conshohocken, PA, USA, (2013).

17. ASTM B328-96. Standard Test Method for Density, Oil Content, and Interconnected Porosity of Sintered Metal Structural Parts and Oil-Impregnated Bearings; ASTM International: West Conshohocken, PA, USA, (2004).
18. T. Gladman, The physical metallurgy of microalloyed steels. Mater. Sci. Technol.,15 (1999) 30-36.
19. T. Gladman, J. Woodhead, The accuracy of point counting in metallographic investigation. J. Iron Steel Inst.,194 (1960) 189-193.
20. M. Marwa, M. B. Anwar and A. Radwan, HBRC Journal, 14 (2018) 379-384.
21. Ö. Özgün, Microstructure and mechanical properties of alloy steels produced by powder metallurgy, Master Thesis Sakarya University Natural and Applied Science Department of Metallurgy and Materials Engineering, Sakarya, Turkey, (2007).
22. L. Ren, J. Zhu, L. Nan, K. Yang, Mater Des., 32 (2011) 3980-3985.
23. T. Shu-ping, W. Zhen-hua, C. Shi-chang, L. Zheng-dong, H. Jie-cai, F. Wan-tang, J. Iron Steel Res Int.,17 (2010) 63-68.
24. Indrani Sen E, Amankwah NS, Kumar E, Fleury K, Materials Science and Engineering: A, 528 (2011) 4491-4499.
25. A. Gaber, A. M. Ali, K. Matsuda, T. Kawabata, T. Yamazaki, S. Ikeno, J. Alloys Compd., 432 (2007) 149-55.
26. Erden, M. A., An Investigation on the Relation Sheep Between Microstructure and Mechanical Properties of Microalloyed Steels Produced by Powder Metallurgy, Ph.D. Thesis, Karabük University Natural and Applied Science Department of Manufacturing Engineering, Karabük, Turkey, (2015).
27. Askeland, D. R. The Science and Engineering of Materials, 1st ed.; Chapman and Hall: London, UK, 1996.
28. S. Takaki, M. Fujioka, S. Aihara, Y. Nagataki, T. Yamashita, N. Sano, Y. Adachi, M. Nomura, H. Yaguchi, Materials Transactions, 45(7) (2004) 2239-2244.
29. M. H. Avazkonandeh-Gharavol, M. Haddad-Sabzevar, A. Haerian, Materials and Design, 30 (2009) 1902-1912.
30. İ. Uygur, J. Fac. Eng. Arch. Gazi Univ., 22(3) 2007 325-330.
31. B. Mishran, K. Kumbhar, K. Siva Kumar, K. Satya Prasad, M. Srinivas, Materials Science and Engineering: A, 651, (2016), 177-183.
32. Yanliang Yi, Jiandong Xing, Mingjia Wan, Langlang Yu, Yafang Lu, Yongxin Jian, Materials Science and Engineering: A, 708 (2017) 274-284
33. M. ES-Souni, E. A. Beaven, G. M. Evans, Materials Science and Engineering: A, 130(2) (1990) 173-84.
34. A. G. Kostryzhev, Al A.Shahrani, C. Zhu, J. M. Cairney, S. P. Ringer, C. R. Killmore, E.V., Materials Science and Engineering: A, 607 (2014) 226-235.
35. T. Siwecki, J. Eliasson, R. Lagneborg, B. Hutchinson, ISIJ Int., 50 (2010) 760-767.
36. W. H. Zhou, H. Guo, Z.J. Xie, C.J. Shang, R.D.K. Misra, Materials and Design, 63 (2014) 42-49
37. Y. R. Wen, A. Hirata, Z. W. Zhang, T. Fujita, C. T. Liu, J. H. Jiang, M. W. Chen, Acta Materialia, 61 (2013) 2133-2147.
38. S. Gündüz, R. Kaçar, Kovove Mater., 46 (2008) 345-350.
39. H. Itow, Y. Nakasaki, G. Minamihaba, K. Suguro and H. Okano, Appl. Phys. Lett., 63 (1993) 934.
40. M. Hajisafari, S. Nategh, H. Yoozbashizadeh, A. Ekrami, J. Iron and Steel Res. Int., 20 (5) (2013) 66.

---

**Сажетак:** У овом раду, испитиван је утицај *С<sub>и</sub>* на микроструктуру, механичка својства и електричну проводљивост челика са додатком *Nb-V*. Узорци микролегура челика су пресовани на 750 МПа и синтеровани на 1400°С у аргону, 1 сат. Величина

зрна и дистрибуција фаза су одређени оптичким микроскопом. Преципитати и површина прелома су анализирани уз помоћ SEM и EDS анализа. Тестови затезања, тврдоће и мерење електричне проводљивости су рађени за легуре са различитим процентом Си. Резултати показују да легура са 10 wt.% Си поседује највише вредности чврстоће и затезања. Међутим, са порастом удела бакра, са 10 на 15 wt.%, обе вредности се смањују. Елонгација такође има тренд смањивања са порастом количине додатог бакра. Иако електрична проводљивост генерално расте са додатком Си, смањење проводљивости је примећено за узорак са 15 wt.% Си.

**Кључне речи:** металургија праха, Nb-V микролегура челика, микроструктура, механичка својства, електрична проводљивост.

© 2022 Authors. Published by association for ETRAN Society. This article is an open access article distributed under the terms and conditions of the Creative Commons — Attribution 4.0 International license (<https://creativecommons.org/licenses/by/4.0/>).

